Available online at www.sciencedirect.com
SCIENCE DIRECT®
Composites Science and Technology 64 (2004) 2501–2507
COMPOSITES SCIENCE AND TECHNOLOGY
www.elsevier.com/locate/compscitech

Monitoring the curing process of epoxy resin nanocomposites based on organo-montmorillonite – a new application of resin curemeter

Dazhu Chen, Pingsheng He *

Department of Polymer Science and Engineering, University of Science and Technology of China, Hefei 230026, Anhui, China

Received 25 September 2003; received in revised form 5 May 2004; accepted 12 May 2004
Available online 15 July 2004

Abstract

Curing of a resin system is the critical and productivity controlling step in the fabrication of thermosetting matrix composites including nanocomposites. In the past few years, in the case of polymer-layered silicate nanocomposites, too many interests were taken in the material structure and properties, while only a few researches were carried on the cure behavior of this type of nanocomposite. The goal of the present work pays mainly attention to the cure kinetics for epoxy resin/organo-montmorillonite (Org-MMT)/2-ethyl-4-methyl-imidazole (2,4-EMI) nanocomposites. The experiments of monitoring curing process of nanocomposite materials are successively made via the *HLX-II* Resin Curemeter. The results derived from the non-equilibrium thermodynamic fluctuation theory indicated that the theoretical prediction is in good agreement with the experimental cure curve. The apparent activation energies were evaluated based on the gel time, t_g and relaxation time, τ, respectively. The increasing of cure temperature accelerated the cross-linking reactions for either nanocomposites or pure epoxy system. The addition of Org-MMT reduces the gel time, t_g as well as the completed cure time, t_c, and increases the rate of cure.

Keywords: A. Nanocomposite; B. Epoxy resin; C. Curing; D. Resin Curemeter; E. Activation energy

1. Introduction

In recent years, nanocomposites, formed when at least one of the phases has a size of 1–100 nm and is well dispersed [1] have attracted considerable attention. Because of their unique phase morphology and their improved interfacial properties, nanocomposites usually exhibit improved physical and mechanical properties (e.g., high strength, modulus and heat distortion temperature) compared with conventional composite materials. One successful method to achieve such nanocomposites is the in situ polymerization of monomer or prepolymer in the interlayer galleries of clay, which was pioneered by the Toyota research group in preparing the nylon 6–clay nanocomposites [2,3]. Following the initial work through in situ interclation and as well as melt interclation on nylon 6 [4,5], many other thermoplastics, such as polypropylene[6], polystyrene [7,8], etc. were included. Besides, epoxy resin, as one of important thermosetting resins has been of great current interest in manufacturing thermoset-based clay nanocomposites with a characteristic of either interclated or exfoliated structure [9–19].

Generally speaking, the forming of various epoxy–clay nanocomposite morphologies is determined by a balance between the intragallery and the extragallery polymerization rates, as discussed by Lan et al. [9]. If the polymerization rate of monomer or prepolymer in the clay layers is lower than the polymerization rate outside, an interclated nanocomposite will form; contrariwise, an exfoliated (or delaminated) structure will be obtained. But often a typical mixture and combination

* Corresponding author. Tel.: +86-551-3601714; fax: +86-551-3601714.
E-mail address: hpsm@ustc.edu.cn (P.S. He).

0266-3538/$ - see front matter © 2004 Elsevier Ltd. All rights reserved.
doi:10.1016/j.compscitech.2004.05.008

of both are observed due to the existence of so-called tactoid, where the layers of clay have been separated by several nanometer or more, but some lateral order of clay is still in existence [10].

During the past few years, majorities of the work concentrated on the forming mechanism of nanocomposite morphology and corresponding physical and mechanical properties [9–15]. The influence of the nature of clay [16], and the structure of cure agent [17], as well as its concentration [18] on the formation of exfoliated nanocomposites have also been examined with efforts. In contrast to this, however, it is seemingly not commensurate in the research on the cure kinetics of resin-based nanocomposites, with only a few publishes [20–22] found. In our present study, we focus on the cure behavior of an epoxy/organo-montmorillonite (Org-MMT) nanocomposite. The natural Na^{+}-montmorillonite was treated via an ion-exchange reaction with one alkylammonium to render the hydrophilic layered silicate organophilic. 2-Ethyl-4-methyl-imidazole (2,4-EMI) was selected as the cure agent of epoxy resin. The structure of the prepared nanocomposite was examined by the X-ray diffraction (XRD) technique and the dependence of the nanocomposite morphology on the cure temperature was also discussed.

The cure behavior of an epoxy–montmorillonite nanocomposite in an isothermal mode was monitored in situ by the *HLX-II* Resin Curemeter developed in our lab. The method, monitoring the cure process with the curemeter is defined as the so-called dynamic torsional vibration method (DTVM) owing to the adoption of a nonresonant forced vibration mode. Differing from the conventional methods (such as DSC, which analyzing the amount of heat evolved isothermally), the DTVM traces directly the change of mechanical properties as a result of the cure reaction and hence it still retains a measurable sensitivity even at the last stage of cure [23]. The application in epoxy resin [21–25] and unsaturated polyester resin [26] polyurethane elastomer [27] and as well as interpenetrating polymer network (IPN) [28] has firmly proved that the DTVM technique is a considerably effective method to study the complicated cure process. In our previous work on the interclated epoxy/montmollonite/methyltetrahydrophthalic anhydride (MeTHPA) nanocomposite [22], the cure data obtained by the DTVM technique were successfully analyzed with Avrami theory of phase change. In this paper, we use another cure model – the nonequilibrium thermodynamic fluctuation theory [29] to analyze the cure behavior of epoxy–montmorillonite–2,4-EMI nanocomposite.

2. Experimental

2.1. The operating principle of HLX-II resin curemeter [23]

As resin cures, the cross-linked density and the viscosity as well as torque (or modulus) of the resin system increase. The resin system with a different degree of cure has a different viscosity (or modulus, viscosity, etc.). Therefore, measuring the changes in torque can realize the monitoring of the degree of cure during the cure process. The homemade *HLX-II* Resin Curemeter (illustrated in Fig. 1) includes three parts: computer system, electronic system and mechanical system. The mechanical system whose sectional view was shown in Fig. 1(a), is the key part for the apparatus to realize its functions. The mechanical part is composed of strain transducer, mold for placing the sample, motor and speed change gear, etc. The electronic system (Fig. 1(b)) serves in amplifying the torque and temperature signals, collecting the state messages of the apparatus and proceeding the A/D tran-

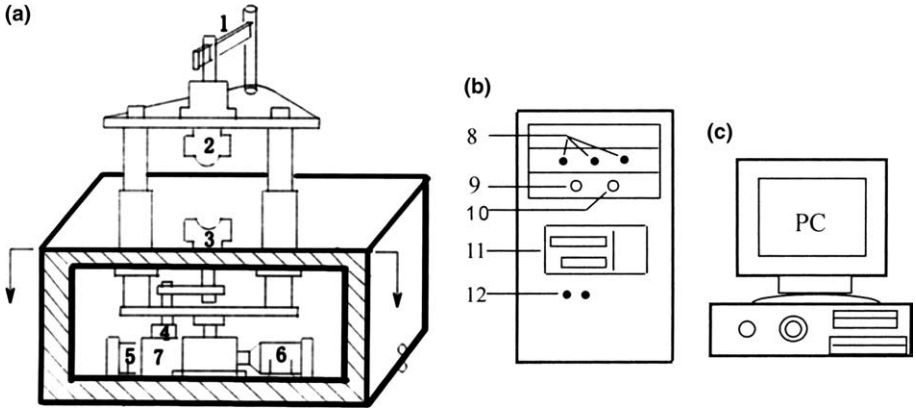

Fig. 1. Schematic representation of the resin curemeter composed of: (a) computer system, (b) electronic system and (c) mechanical system. (1) strain gauge load cell, (2) upper mold, (3) lower mold, (4) eccentric disc, (5) motor for torsional vibration, (6) motor for closing molds, (7) speed change gear, (8) indication lamp marking the work state of up-and-down motor and amplifier, (9) zero adjust knob, (10) magnification times option knob, (11) temperature control meter and (12) indication lamp for main electric power supply.

sition, which makes it possible for the computer system to collect system states and data and thereby control the whole curemeter. Its hardcore is made up of amplifier, A/D converter, temperature controller and interface control unit. The computer system (Fig. 1(c)) is responsible for sending commands to control each operation of the curemeter. With the aid of a self-programming software, the recordation and treatment of data is completed efficiently through this part.

The resin curemeter used adopts the mode of dynamic torsional vibration belonging to a nonresonant forced vibration. The resin mixture is placed in the lower mold 3 used as the torsional vibrator. When the motor 6 is switched on, the upper mold 2 comes down, and the molds close with a gap that can be adjusted. Before this operation, the two molds are heated to an appointed temperature via the heater within them and keep constant temperature at least half an hour for performing the isothermal tests. As soon as the molds close, the motor 5 is turned on, and the lower mold starts a torsional vibration at an angle below 1°, which also can be adjusted according to the hardness of cured resin materials, by means of eccentric disc 4 on the speed change gear 7. The torque amplitude of the torsional vibration is transformed into electric signals by means of the strain gauge load cell 1. After amplified through the electronic system, the electric signals are recorded by the computer, and as the result, the resin cure process is timely monitored.

2.2. Materials and preparation of the epoxy resin/montmorillonite nanocomposite

The diglycidyl ether of biphenyl A, epoxy resin *E*-51 with the epoxy value 0.48–0.54 and average epoxy equivalent 196, was produced by Shanghai Resin Factory. 2,4-EMI supported by the Development Center of Special Chemical Agents in Huabei Region, was used as the curing agent. The raw Na^+-montmorillonite (MMT) with the cation exchange capacity (CEC) value of 100 meq/100 g clay, was purchased from QING SHAN Chemistry Agent Factory in LIN AN, China. The Org-MMT was prepared by an ion exchange reaction between Na^+-montmorillonite and $CH_3(CH_2)_{15}$-$N(CH_3)_3Br$ according to the method given in the document [17]. The treated montmorillonite with a size <53 μm was collected.

In the case of multi-component nanocomposite system, the order of mixing of the initial materials, processing conditions and curing temperatures affect as usual the ultimate structure of nanocomposite [10]. For this experiment, the mixing of the three components included two steps: (1) A relatively low-viscosity epoxy prepolymer was mixed with 0, 5 and 10 phr (parts per hundred resins) Org-MMT, respectively, followed by a thoroughly stirring for about 5 min at room temperature. This process facilitated the insertion of epoxy molecules into the montmorillonite galleries, ensuring a sufficient swelling. (2) The cure agent, 2,4-EMI with a state of super-cooling liquid was added into the epoxy–Org-MMT mixture. The concentration ratio of epoxy resin and 2,4-EMI was fixed at 100:5 by weight. After a fully stirring process, about 1.5 g of the three-component mixture were cast into the lower steel mold for isothermal curing in situ. When the higher mold descends and closes to the lower, the curing reaction was initiated at once. The curing temperatures used ranged from 70 to 85 °C. For each of isothermal DTVM experiments, the curing process was preceded until the curemeter could not examine the increasing of torque of the resin system.

2.3. Characterization by XRD

X-ray diffraction patterns were recorded by monitoring the diffraction angle 2θ from 1.5° to 10° on a Rigaku-D/max-γA X-ray diffractometer. The diffractometer was equipped with a Cu Kα ($\lambda=0.154$ nm) radiation source operated at 40 kV and 100 mA. The scanning speed and the step size used were 2°/min and 0.02°, respectively.

3. Results and discussion

3.1. XRD characterization

To verify that the epoxy prepolymer enters the clay galleries and an epoxy resin/Org-MMT nanocomposite was formed, the cure process at various temperatures was followed by XRD characterization (Fig. 2). The diffraction angle for (0 0 1) reflection of raw MMT is 7.01°, and the corresponding interlayer spacing is 1.26 nm ac-

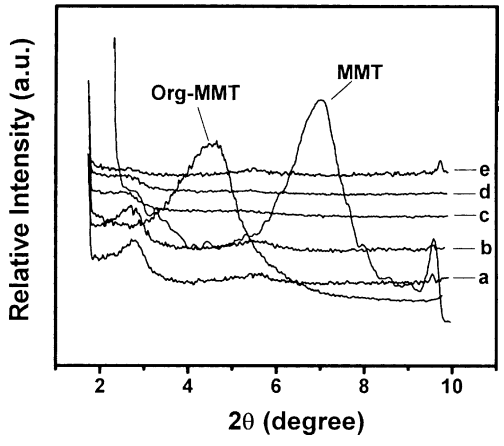

Fig. 2. The XRD patterns for MMT, Org-MMT and epoxy resin E51/Org-MMT/2,4-EMI nanocomposites cured at: (a) 65, (b) 70, (c) 75, (d) 80 and (e) 85 °C.

cording to Bragg's law ($\lambda = 2d\sin\theta$). As a result of the modification with long-chain alkylammonium salt, the diffraction angle for (0 0 1) peak of Org-MMT drops to $2\theta = 4.64°$ and the corresponding interlayer spacing increases to 1.90 nm. The position of the major peak assigned to the basal plane (0 0 1) of the silicate. If this peak is still present then intercalation, however when missing then exfoliation of the organo-clay occurred. The presence of this peak at $2\theta < 5.0°$ with broad width should indicate for a combined intercalation/exfoliation process [30].

Fig. 2 demonstrates that different cure temperatures lead to various degrees of exfoliation of Org-MMT at a given Org-MMT loading. When the epoxy resin was cured at 65 or 70 °C, a clear (0 0 1) diffraction was observed, indicating a typical interclated structure formed. The interlamellar spacing in this interclated nanocomposite is about 3.22 nm corresponding to a (0 0 1) diffraction angle of 2.74°. However, interestingly when higher cure temperature was applied, the diffraction peak weakened, and a trend to shifting towards lower angle was examined, followed by an increase in *d*-spacing of Org-MMT. To date, at 85 °C, the (0 0 1) reflection has become not obvious. The findings reveal that the degree of exfoliation of the Org-MMT improved with increasing cure temperature and as a result both intercalated aggregates and exfoliated platelets are covered. The dependence of exfoliation of the clay on the cure temperature was also examined by Giannelis [11] Tolle [31] and Kornmann [17]. A balance between the intragallery and the extragallery polymerization rates controls the exfoliation of the clay in epoxy system [9] as mentioned above. Higher cure temperature increases not only the reactivity of the epoxy system, but also the diffusion rate of the epoxy and the curing agent, favoring the intragallery cure kinetics. This results in a higher degree of exfoliation of the clay.

3.2. General introduction to the experimental cure curve

To clearly understand the experimental isothermal cure curve derived from the *HLX-II* Resin Curemeter, a classic curve for epoxy matrix obtained at 80 °C shown in Fig. 3 is taken for illustration. The abscissa in Fig. 3 is the curing time and the ordinate is the torque required to turn the resin system by a small angle, which corresponds to the modulus or viscosity of the resin system, and can be thought of as a relative parameter of the degree of cure. The time of closure of the molds is taken as the starting time of cure (i.e. the point *O*). In the range of *OA* of the curing time the cross-linked network structure formed during the cure is not enough to cause forced vibration of the upper mold. As a result, the strain gauge load cell will not have any signal to input, so that the experimental curve is linear corresponding to the abscissa. At the point *A*, the viscosity of the resin

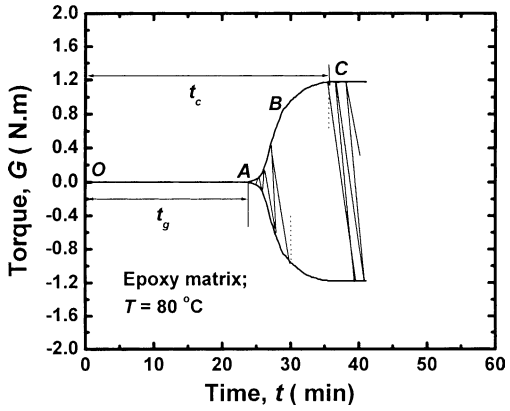

Fig. 3. General introduction to the experimental isothermal cure curve analysis.

system is high enough (i.e., the cross-linking network formed is complete enough) for the gelation in the resin system to occur, and the torque appears. The strain gauge load cell inputs some signal. Thus, the time from the starting point *O* to point *A* is defined as the gel time t_g for the resin system. After point *A* the torque increases with increasing of curing time. Point *B* represents any point at the experimental cure curve. The increasing amplitude of the torque (slope of the *OB* curve) expresses the rate of the curing reaction. The increasing trend of torque tends to steady with increasing curing time, and the equilibrium torque G_∞ is thus reached (point *C*). The curing reaction is completed and the cup-shaped experimental curve is obtained. The time corresponding to *OC* is the full curing time t_c. Since the experimental cure curve is strictly symmetrical, it is reasonable to take its upper envelope as the cure curve for common analysis of cure data.

3.3. Isothermal cure curves of epoxy resin and the nanocomposites

The isothermal cure curves of pure epoxy E51/2,4-EMI system without any Org-MMT at 70, 75, 80 and 85 °C obtained by the DTVM are shown in Fig. 4(a). The curves are similar in shape at different temperatures. The gel times t_g can be easily read from the curves directly. The t_g for the system cured at 70 °C is 48.9 min, and they decrease with increasing of the temperature. The t_g for the system cured at 85 °C has been down to 15.0 min. The initial torque G_0 is zero because the curve at the time range from 0 to t_g is identical to abscissa. After the gel time t_g the torque appears and the increasing amplitude of torque increases with increasing of the temperature. The slope of the curve after t_g reflects the cure rate, and it means that the cure rate increases with increasing of the temperature. All these facts agree with the general law of the dependence of cure rate on reaction temperature. The time reaching

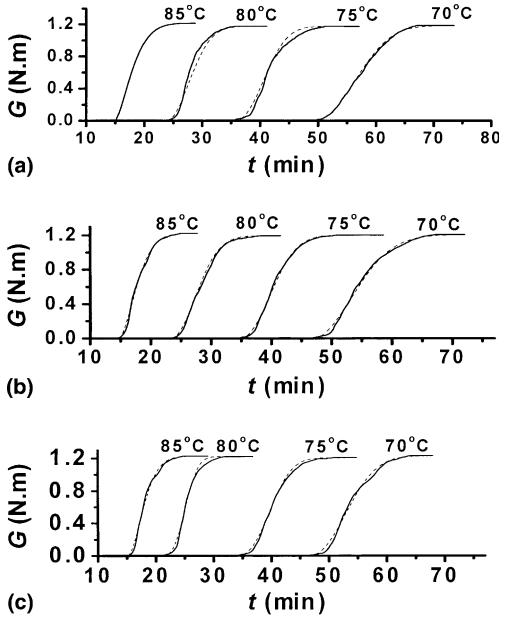

Fig. 4. Plots of torque vs. time for epoxy resin E51/Org-MMT/2,4-EMI nanocomposites with Org-MMT loadings of: (a) 0, (b) 5 and (c) 10 phr. (——) Experimental; (·····) theoretical.

the maximum or equilibrium torque G_∞ is the completed cure time t_c, which also decreases with increasing of the temperature, but the G_∞ is almost same for these four temperatures. The values of t_g and t_c at four temperatures for pure resin systems are listed in Table 1.

Fig. 4(b) and (c) shows the isothermal cure curves of epoxy resin E51/Org-MMT /2,4-EMI nanocomposite with two Org-MMT loadings of 5 and 10 phr. The isothermal cure curves with or without Org-MMT are similar in shape as well. The increasing amplitudes of torque (corresponding to the rate of cure) for nanocomposites are almost the same as that of pure resin system, but the gel times and the completed cure times for nanocomposites decrease with increasing of the Org-MMT loading in nanocomposites, which indicates that the addition of Org-MMT has a some effect on enhancing the gelation as well as the total cross-linking reaction. For example, the epoxy system at 5 phr loading cured at 70 °C has a decrease of 2.3 min in t_g comparing with the pure one. This may attribute to that the Org-MMT provides a surface area large enough to ensure the adsorption and dispersion of the reactants, and in addition the alkylammonium (the treating agent of inorganic montmorillonite) has some catalysis effect on the cure reaction [10,21,22].

The cure behavior of epoxy resin E51/Org-MMT/2,4-EMI nanocomposite has an evident temperature dependence in the same way. With increasing cure temperature, the cure reaction is accelerated and the slope of the cure curve is increased. As the result, the values of t_g and the completed cure time t_c decrease markedly.

3.4. Application of Flory's gelation theory

According to Flory's gelation theory [32], the chemical conversion at the get point of the resin system is constant and is not related to the reaction temperature and experimental conditions. As a result, the apparent activation energy ΔE_a of cure reaction can be calculated from the gel time t_g:

$$\ln t_g = C + \frac{\Delta E_a}{RT}, \tag{1}$$

where C is a constant, R is the gas constant and T is the absolute temperature of cure. Fig. 5 shows a plot of $\ln t_g$ against $1/T$ for various amounts of Org-MMT. The good linear relationship indicates that the relationship between t_g and T has been a good agreement with Flory's gelation theory. The apparent activation energies, calculated from the slope of the line have the value of 80.1–82.2 kJ/mol shown in Table 1. The cure kinetic parameters of pure epoxy/2,4-EMI system have been

Table 1
The cure kinetic parameters for the pure epoxy resin and the nanocomposites

Org-MMT (phr)	T (°C)	t_g (min)	t_c (min)	β	ΔE_{a1}[a] (kJ/mol)	ΔE_{a2}[a] (kJ/mol)
0	70	48.9	68.2	2.26		
	75	35.5	51.2	2.27	82.2	64.8
	80	23.8	35.6	2.03		
	85	15.0	26.7	1.53		
5	70	46.6	67.3	1.94		
	75	34.5	50.5	2.16	80.4	60.4
	80	23.3	37.2	2.00		
	85	14.6	24.7	1.72		
10	70	46.4	64.1	2.23		
	75	33.9	50.1	2.48	80.1	70.0
	80	21.1	31.9	2.74		
	85	14.8	24.5	1.74		

[a] ΔE_{a1} and ΔE_{a2} are the activation energies obtained by Flory's theory and the nonequilibrium thermodynamic fluctuation theory, respectively.

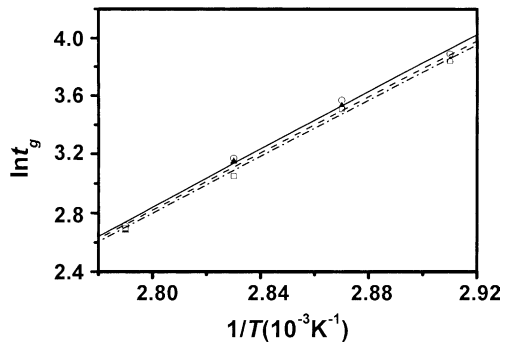

Fig. 5. Plots of $\ln t_g$ vs. $1/T$ for epoxy resin E51/Org-MMT/2,4-EMI nanocomposites with different Org-MMT loadings. (—○—) 0 phr; (––▲––) 5 phr; (–·–□–·–) 10 phr.

obtained using DSC method by Berger and Lohse [33] with the ΔE_a value of 80.3 kJ/mol. As expected, the kinetic parameter ΔE_a obtained by DSC method and DTVM match very well.

3.5. Analysis of nonequilibrium thermodynamic fluctuation theory

About twenty years ago, Hsich [29] proposed that there is a similarity between the cure kinetic process and the molecular structural relaxation process based on the concept of nonequilibrium thermodynamics. According to this point of view, the curing reaction can be considered as a multiple chemical reaction in which each chemical reaction is associated with a thermodynamic ordering parameter ε_i. Thus variations in physical or mechanical properties during cure can be expressed as the time correlation of the mean square fluctuation of ordering parameters:

$$\frac{G_\infty - G_t}{G_\infty - G_0} = \sum_i W_i(\Delta\varepsilon_i)^2 \exp\left[-\left(\frac{t}{\tau_i}\right)\right]. \tag{2}$$

Let

$$g_i = W_i(\Delta\varepsilon_i)^2. \tag{3}$$

Then

$$\frac{G_\infty - G_t}{G_\infty - G_0} = \sum_i g_i \exp\left[-\left(\frac{t}{\tau_i}\right)\right], \tag{4}$$

where G_0 and G_∞ are respectively the initial and final physical or mechanical properties during cure, G, is the properties at time t, $(\Delta\varepsilon_i)^2$ is the mean square fluctuation of the ordering parameter ε, W_i and g_i are the weight constants, and τ_i, is the relaxation time of the reaction system correlated with the ordering parameter ε_i. Based on the normalization of $\sum_i g_i = 1$ and a generation from a sum of single relaxation processes to a continuous distribution of such processes, the physical or mechanical properties (such as torque) of resin system can be expressed as

$$\frac{G_\infty - G_t}{G_\infty - G_0} = \exp\left[-\left(\frac{t - t_g}{\tau}\right)^\beta\right], \tag{5}$$

where β is the constant describing the width of the relaxation spectrum.

In our experiment the mechanical property involved is torque. As seen from the isothermal cure curve in Fig. 4, G_0 is zero; the torque begins to appear only after the gel time t_g. Eq. (5) describing the cure curve after t_g may be written as

$$\frac{G_\infty - G_t}{G_\infty} = \exp\left[-\left(\frac{t - t_g}{\tau}\right)^\beta\right] \tag{6}$$

or

$$G_t = G_\infty\left\{1 - \exp\left[-\left(\frac{t - t_g}{\tau}\right)^\beta\right]\right\}. \tag{7}$$

Apparently, Eq. (7) characterizes the change of torque of the system with the cure time.

In order to obtain the relaxation time τ, let $t = t_g + \tau$, thus

$$G_{t=t_g+\tau} = G_\infty(1 - e^{-1}) = 0.63G_\infty. \tag{8}$$

Hence, the relaxation time τ can be obtained by a measurement of the time corresponding to $G = 0.63G_\infty$ in the cure curve, followed by a simple calculation according to the equation $\tau = t - t_g$.

The relationship between the relaxation time and the cure temperature is in accordance with Arrhenius equation [29]

$$\ln\tau = \ln\tau_0 + \frac{\Delta E_a}{RT}. \tag{9}$$

From the slope of the linear fit in the $\ln\tau \sim 1/T$ plot (Fig. 6), the apparent activation energy ΔE_a can also be easily got. The values of ΔE_a (listed in Table 1) for the cure systems filled with different Org-MMT loading remain in the range of 60.4–70.0 kJ/mol, which is near to that calculated by Flory's gelation theory.

After the τ value determined, Eq. (7) is reduced to an equation with a single parameter β only. A method of

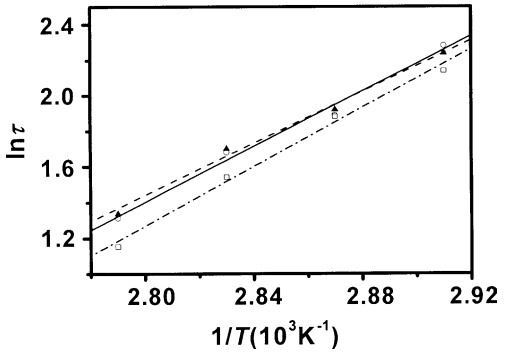

Fig. 6. Plots of $\ln\tau$ vs. $1/T$ for epoxy resin E51/Org-MMT/2,4-EMI nanocomposites with different Org-MMT loadings. (—○—) 0 phr; (––▲––) 5 phr; (–·–□–·–) 10 phr.

nonlinear least squares was used to fit Eq. (7) to all experimental cure curves. The values of β (Table 1) at various curing temperature and Org-MMT loadings can be determined using the line of best fit. The values of β are larger than 1.0 indicate that the cure reaction is not a simple first-order but a high-order chemical reaction [28]. With the obtained values of β, t_g and τ, the torque G for any time, i.e., the theoretically predicted value, can be calculated according to Eq. (7). The theoretical curves (broken lines) are also plotted in Fig. 4. Obviously, the theoretical prediction shows a good agreement with the experimental cure curves for epoxy system with or without Org-MMT.

4. Conclusions

The cure behavior of epoxy resin E51/Org-MMT/2,4-EMI nanocomposites was investigated by using the *HLX-II* Resin Curemeter. The conclusions are as follows:

1. When relatively lower cure temperature is applied, a typical interclated nanocomposite is obtained; with increasing the cure temperature, the degree of exfoliation of the Org-MMT is improved and often a combination of both interclated and exfoliated structure can be observed.
2. The addition of Org-MMT increases the rate of curing reaction with a reduction of the gel time t_g and the completed cure time t_c. With increasing of temperature the values of t_g and t_c decrease for any cure system.
3. The Flory's gelation theory and non-equilibrium thermodynamic fluctuation theory can be used to examine the cure behavior of epoxy resin E51/Org-MMT/2,4-EMI nanocomposites. And the results approve that the non-equilibrium thermodynamic fluctuation theory can be used to predict the cure process using limited experimental data.

References

[1] Giannelis EP. Adv Mater 1996;8:29–35.
[2] Kojima Y, Usuki A, Kawasumi M, Okada A, Fukushima Y, Kurauchi T, et al. J Polym Sci A 1993;31:983–6.
[3] Usuki A, Kojima Y, Kawasumi M, Okada A, Fukushima Y, Kurauchi T, et al. J Mater Res 1993;8:1179–83.
[4] Liu LM, Qi ZN, Zhu XJ. J Appl Polym Sci 1999;71:1133–8.
[5] Vander Hart DL, Asano A. Macromolecules 2001;34:3819–22.
[6] Xu WB, Ge ML, He PS. J Polym Sci B 2002;40:408–14.
[7] Vaia RA, Jandt KD, Kramer EJ, Giannelis EP. Macromolecules 1995;28:8080–5.
[8] Fu X, Qutubuddin S. Polymer 2001;42:807–13.
[9] Lan T, Kaviratna PD, Pinnavaia TJ. Chem Mater 1995;7:2144–50.
[10] Brown JM, Curliss D, Vaia RA. Chem Mater 2000;12:3376–84.
[11] Messersmith PB, Giannelis EP. Chem Mater 1994;6:1719–25.
[12] Lan T, Pinnavaia TJ. Chem Mater 1994;6:2216–9.
[13] Wang Z, Lan T, Pinnavaia TJ. Chem Mater 1996;8:2200–4.
[14] Lee DC, Jang LW. J Appl Polym Sci 1998;68:1997–2005.
[15] Hsiue GH, Liu YL, Liao HH. J Polym Sci A 2001;39:986–96.
[16] Kornmann X, Lindberg H, Berglund LA. Polymer 2001;42:1303–10.
[17] Kornmann X, Lindberg H, Berglund LA. Polymer 2001;42:4493–9.
[18] Chin IJ, Thurn-Albrecht T, Kirn HC, Russell TP, Wang J. Polymer 2001;42:5947–52.
[19] Zerda AS, Lesser AJ. J Polym Sci B 2001;39:1137–46.
[20] Butzloff PB, Dsouza NA, Golden TD. Polym Eng Sci 2001;41:1794–802.
[21] Xu WB, He PS, Chen DZ. Eur Polym J 2003;39:617–25.
[22] Chen DZ, He PS, Pan LJ. Polym Test 2003;22:689–97.
[23] He PS, Li CE. Modern Scientific Instrument (Chin) 1999;6:17–20.
[24] He PS, Li CE. J Mater Sci 1989;24:2951–6.
[25] He PS, Li CE. J Appl Polym Sci 1991;43:1011–6.
[26] He PS, Zhou ZQ, Li CE. Acta Mater Compos Sinica 1985;2(3):81–3.
[27] He PS, Li CE, Liu YL, Ruan DL. Rubber Industry (Chin) 1984;8:41–3.
[28] Huang FH, Li CE, He PS, Zhang YC, Ruan DL. Polym Mater Sci Eng 2000;17(1):93–7.
[29] Hsich HS-Y. J Appl Polym Sci 1982;27:3265–77.
[30] Mousa A, Karger-Kocsis J. Macromol Mater Eng 2001;286:260–6.
[31] Tolle TB, Anderson DP. Compos Sci Technol 2002;62:1033–41.
[32] Flory PJ. Principles of polymer chemistry. New York: Cornell University Press; 1953.
[33] Berger J, Lohse F. J Appl Polym Sci 1985;30:531–46.